Investigated the effects of surfactant concentration on cobalt ferrite nanoparticles synthesized in reverse micelles

K. Devy[a,b], M. Murugan[a,*], G.S.V.R.K. Choudary[c], M. C. Varma[d]
[a]*Department of Physics, Government Arts College (Affiliated to Bharathidasan University), Tiruchirappalli, Tamilnadu, 620022, India*
[b]*Department of Physics, St. Francis College for Women, Hyderabad, Telangana, 500016, India*
[c]*Department of Physics, Bhavan's Vivekananda College of Science, Humanities and Commerce, Hyderabad, Telangana, 500094, India*
[d]*Department of Physics, School of Science, GITAM University, Vishakhapatnam, Andhra Pradesh 530045, India*

The use of reverse micelles as nanoscale hydrophilic voids of microemulsions in the manufacture of ferrites has been recognized since the 1960s, but there has been very little attention on the structural and magnetic properties with respect to surfactant concentration. This paper investigates the influence of surfactant sodium dodecyl sulphate (SDS) concentrations on cobalt ferrite ($CoFe_2O_4$) nanoparticles prepared by reverse micelles at annealing temperatures 250°C and 500°C. Samples with varied cobalt to SDS ratios (Co: SDS = 1: 0.33, 1: 0.5, 1: 0.66) were subjected to XRD, TGA, TEM, FTIR and VSM Studies. All the samples exhibited single-phase spinel structures with crystalline diameters ranging from 10 to 18 nm. As the SDS concentration increased the crystallite size decreased. The TEM images showed the particle size in the range of 7.6 -17.7 nm. VSM investigations show the ferromagnetic behavior of the sample. The observed increase in coercivity with respect to annealing temperature for the same concentration reflects the single-domain nature of the nano particles. This underscores the crucial role of annealing conditions in customizing cobalt ferrite nanoparticles as a suitable application in longitudinal magnetic recording media.

(Received March 26, 2024; Accepted June 7, 2024)

Keywords: Cobalt to SDS ratio, Particle size, Reverse micelles, Sodium dodecyl sulphate

1. Introduction

Ferrite magnetic nanoparticles have always remained as one of the most intensively researched and studied materials for its wide applications, including ferrofluid technology, magnetic refrigeration, magnetic resonance imaging (MRI), high-density recording, spintronics, anti-tumor drug delivery, magnetic hyperthermia, and others [1-4]. Cobalt ferrite nanoparticles have garnered a lot of interest because of their mixed spinel structure, which contains divalent cobalt cations and trivalent ferric cations at A and B sites in the lattice [5]. Cobalt ferrite ($CoFe_2O_4$) possesses remarkable physical and mechanical properties, as well as being exceptionally chemically stable and electrically insulating [6,7]. These exceptional characteristics make cobalt ferrite a viable contender for a broad range of medical applications [8].

The goal of various methods for synthesizing ferrite nanoparticles is to match their features, such as particle size and distribution, shape, degree of agglomeration, and particle composition, to specific applications. Controlling these qualities allows you to improve the performance of nanoparticles in a variety of applications, including magnetic data storage, biological imaging, catalysis, and environmental cleanup. Sol-gel [9], co-precipitation [10], microemulsion [11], and other popular methods that are used, have their advantages and limitations.

* Corresponding author: manickmurugan68@gmail.com
https://doi.org/10.15251/DJNB.2024.192.889

As each feature is tied to the characteristic length scale, particle size is an important parameter in changing the properties. Bottom-up techniques employ chemical processes to create nanoparticles from atomic or molecular precursors, allowing the precursor particles to grow. The key to getting the correct chemical and physical qualities is to stop or slow the growth of particles to the desired size. Improved particle size control, dispersity, homogeneity, and low energy usage are further advantages of reverse micellar synthesis over previous bulk and wet techniques [12].

Reverse micelle method was used to prepare nano particles of cobalt ferrite at varying concentrations of SDS. In this method, different reactants are added to two separate microemulsions consisting of the following- surfactant, cosurfactant, oil-phase liquid, and water (aqueous solution). The surfactant acts as a separating layer, which is referred as an interface, and is a medium between the polar water and non-polar oil phases. In the reverse micelle method, the surfactant forms a spherical shell microstructure between these two phases, in which a small amount of water is dispersed in the oil phase. The micelle size is controllable by adjusting the volume of surfactant and water. Inside the micelle, the presence of water is vital in the formation of nanoparticles, acting as a confined reaction environment. Reverse micelle which are of small size, limits the diffusion of reactants, and determines the way in which the size and shape of the nanoparticle is formed [13-18].

2. Materials and preparatory methods

Cobalt nitrate hexahydrate [Co $(NO_3)_2.6H_2O$], Iron nitrate hexahydrate [Fe $(NO_3)_2.6H_2O$], Sodium dodecyl sulphate salt (SDS), n-Hexane (99%), 1-Butanol of analytical grade HIMEDIA was utilized without any additional purification. The precursor solution is obtained by dissolving the metal nitrates in the required proportions distinctly in the relevant amount of deionized water, then mixing and stirring for an hour, which is then used for the following processing technique.

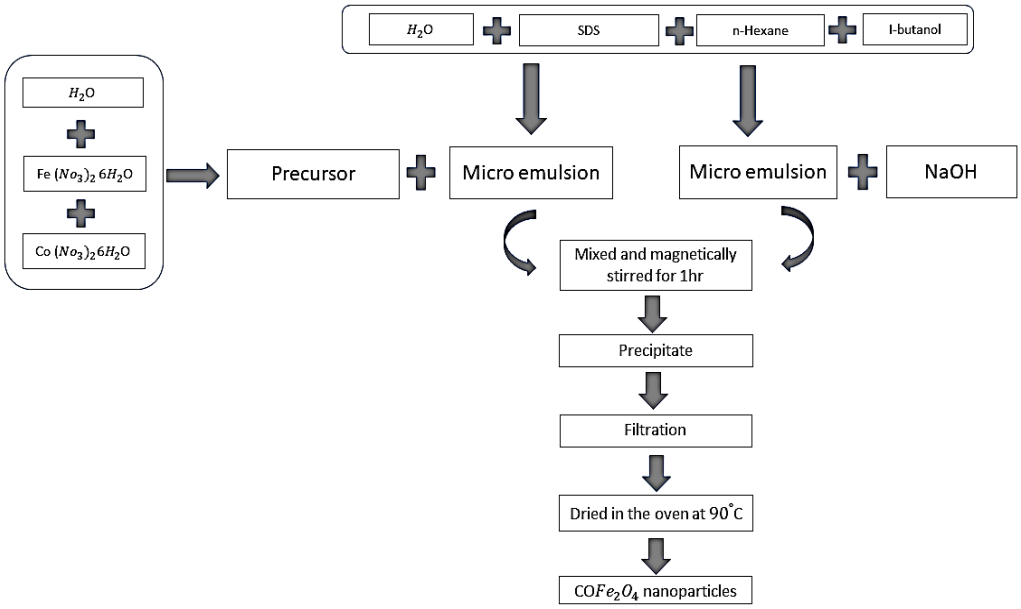

Fig. 1. Schematic representation of reverse micelle synthesis of Cobalt Ferrite nanoparticle.

We created two micro-emulsion systems using the reverse micelle approach (Fig. 1) by mixing the following – SDS, water, 1-butanol, and n-hexane in the appropriate ratios. After one hour, we observed a stable micelle formed with a clear, transparent. In one of the micro-emulsion systems, we dissolved the precursor solution, also we added 5M NaOH (reagent) solution to the

other micro-emulsion. The two resulting microemulsions were combined and magnetically swirled for an hour. Within the reverse micelle nanoreactors, cobalt ferrite is precipitated. Then to eliminate the water content, we dried the resultant substance for a period of 6 hours at 90 °C in a hot air oven[19-20]. For further investigation, the dried powder (as-prepared sample) was homogeneously mixed in the agate mortar for 10 minutes using a pestle. To test the impact of SDS, samples with varied cobalt to SDS ratios (Co: SDS = 1: 0.33, 1: 0.5, 1: 1) were used.

3. Results and discussions

The sample (Co-to-SDS ratio of 1:0.5) was subjected to an XRD study to ascertain whether the intended material was obtained. Peaks of 111, 311, 400 and 440 observed in the XRD pattern (Fig. 2) shows the commencement of ferrite formation, and the noise present in the XRD pattern suggests a need for improvement of the crystallization process through further heat treatment. The presence of wider peaks denotes the particles are very fine and the noisy pattern represents the amorphous nature present in the sample. To increase the crystallinity further heat treatment is necessary [21,22].

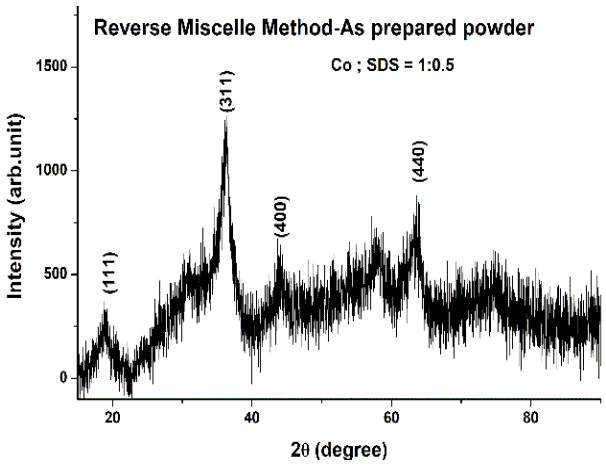

Fig. 2. Cobalt ferrite(as-prepared) XRD pattern.

To identify the temperatures at which the crystallization is completed and ferrite formed, DTA and TGA studies were conducted on the samples.

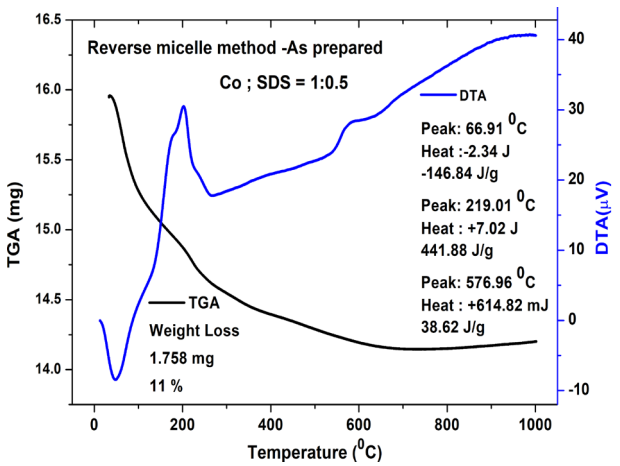

Fig. 3. TGA & DTA pattern of as-prepared cobalt ferrite.

To generate breakdown profiles, the material underwent heating in a nitrogen atmosphere starting from 32°C and reaching 1000°C at a rate of 10°C/min. The sharp weight loss of the sample from 32°C to 250°C in the curve of TGA is associated with the endothermic peak at 67°C, and it gradually decreases till 700°C, and there is found to be no further loss of weight after 700°C. The endothermic peak below 100°C is attributed to the removal of the solvent. Exothermic peak observed at 240°C is attributed to the removal of the surfactant and the OH group. While exothermic peak observed at 570°C is because of the crystallization of the amorphous to a cubic phase of $CoFe_2O_4$[23].

Fig. 4 (a to c), shows the FTIR spectrum of all samples in 4000-400 cm^{-1} range. As per our observation, the band around 593 cm^{-1} is due to the stretching vibrations of the (M_{tet} -O) bond at the tetrahedral site [24]. Due to the limitations of the instrument, the octahedral site (M_{oct}-O) bond is not seen properly.

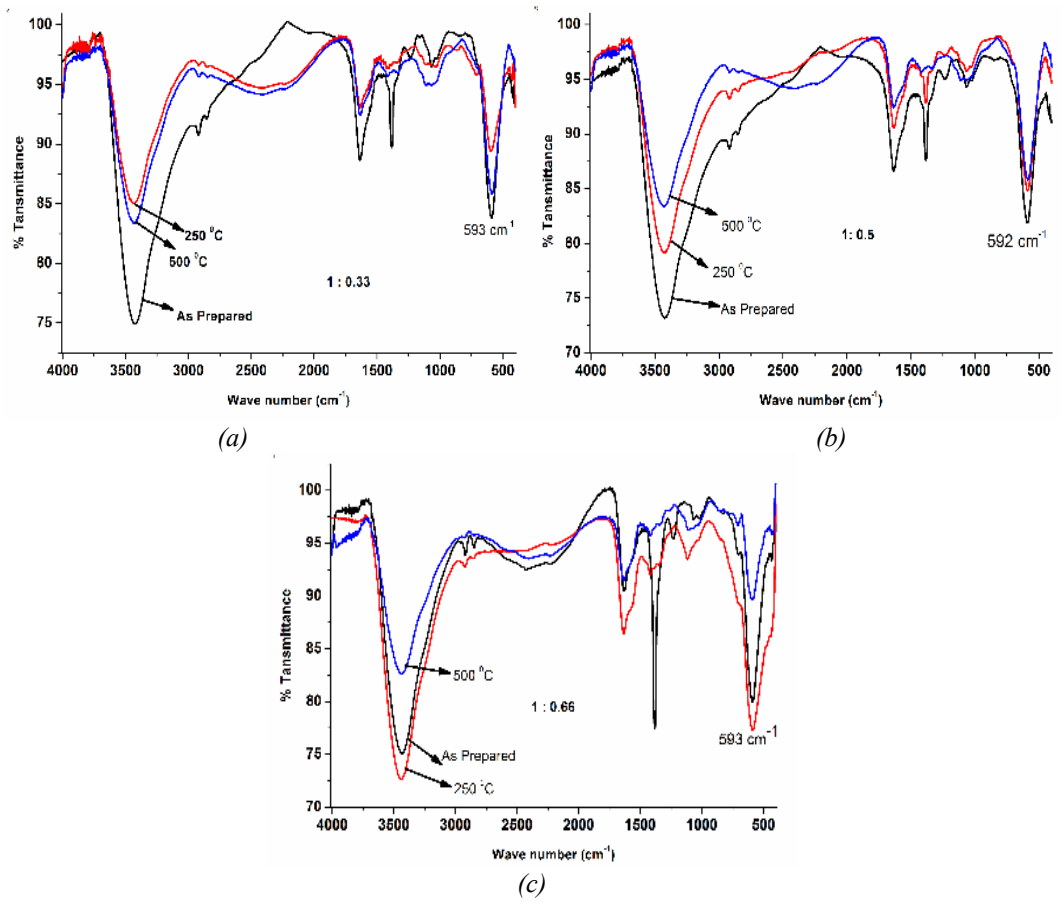

Fig. 4. (a-c) FTIR spectra of Cobalt Ferrite samples with different SDS concentration.

The absorption band observed around 3430 cm^{-1} and 1600 cm^{-1} are the result of vibrations of (O-H) stretching mode and (H-O-H) bending mode [25,26].These bands are found to decrease in intensity after heating in all three as-prepared samples . We also note that aliphatic (C-H) species stretching mode results in the weak band at 2910 cm^{-1}. The absorption band at 1060 cm^{-1} is assigned to -S=0 stretching vibrational modes of sulphonic acid group present in SDS [27,28].

Notably, no significant shift in wave number corresponding to the tetrahedral site points out to the possibility of no change in cation distribution with variation in SDS content. The FTIR spectra analysis shows that cobalt ferrite nanoparticles may be synthesized using the reverse micelle approach with various SDS concentrations and proving that heating has an effect on the prepared samples.

Fig. 5a, and 6a show the X-ray diffraction (XRD) for the synthesized samples of cobalt ferrite nanoparticle with ratio Co: SDS=1:0.33, 1:0.5, and 1:0.66 at annealing temperatures of 250□C and 500□C , and observed that all the peaks represent spinel ferrite structure (JCPDS PDF #221086) [29]. The peaks are observed to be more intense and narrower as the annealing temperature is increased. The increase in annealing temperature may have improved the crystallinity. We also used FullProf software based on the $Fd\bar{3}m$ space group to analyze the XRD data by the Rietveld refinement method.

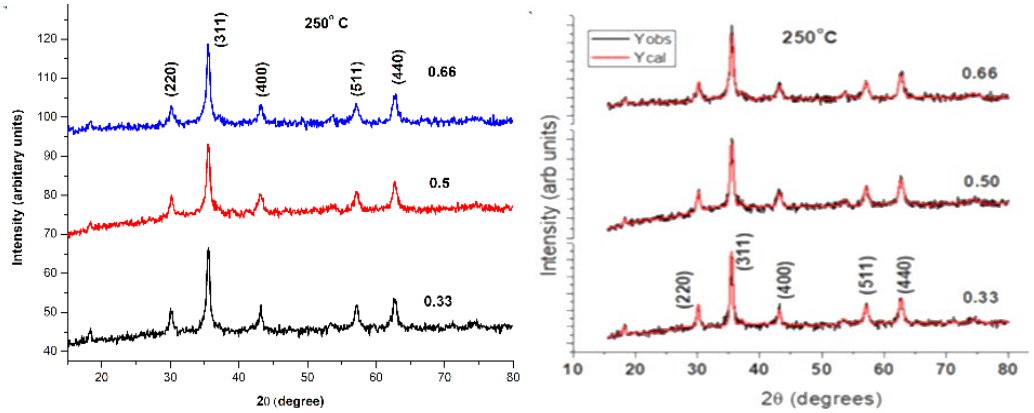

(a) (b)

Fig. 5. (a) Cobalt Ferrite XRD pattern with varying concentration of SDS at 250 ℃. (b) Rietveld refinement pattern of Cobalt Ferrite with varying concentration of SDS at 250 ℃.

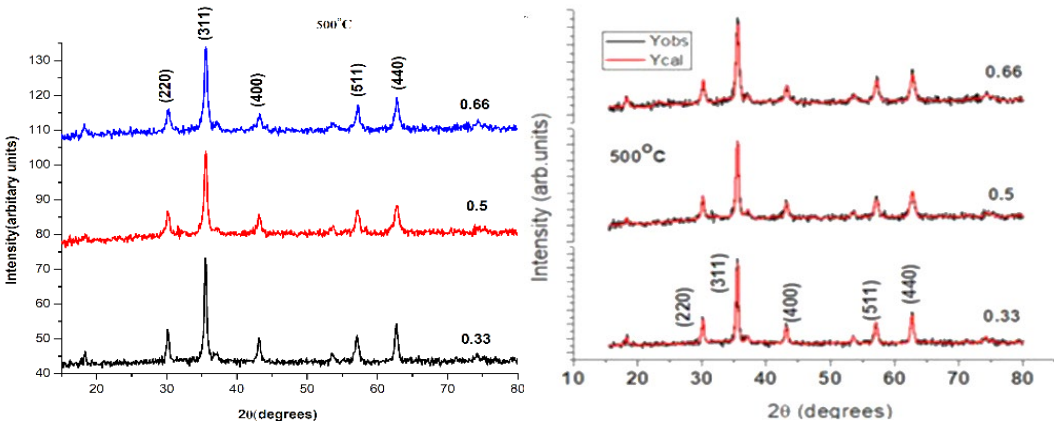

(a) (b)

Fig. 6. (a) Cobalt Ferrite XRD pattern with different SDS concentration at 500 ℃. (b) Rietveld refinement pattern of Cobalt Ferrite with varying concentration of SDS at 500 ℃.

The unit cell volume (V), X-ray density (d_x), specific surface area (S) and Crystallite size (D) by the Scherer equation [30] are calculated by the following expression:

$$V = a^3 \tag{1}$$

$$d_x = \frac{ZM}{N_A V} \tag{2}$$

$$S = \frac{6}{d_x D} \tag{3}$$

$$D = \frac{k\lambda}{\beta \cos\theta} \quad (4)$$

where Z = 8, M, N, A are the number of molecules per unit cell, molecular weight for each sample, Avogadro's number, k is the Scherer factor (0.9), β is the full width half maximum (FWHM), and λ = 1.5406 ° A is the wavelength of X-rays used for recording the diffraction patterns.

Table 1 values agree with previously declared studies of cobalt ferrite, which approve the formation of spinel structure with good densification [31]. Crystallite size obtained from the FWHM of a diffraction peak may include the effects of micro strain and instrumental broadening. Separation of the size and strain components can be done using the Williamson-Hall plots (W-H plots) [32,33]. The crystallite size estimated from the W-H plot as displayed in Table 1 looks to be more precise because of making the strain component zero. Also, the Table 1 values corroborated that with the increase in SDS concentration the crystallite size decreases. Surfactant concentration may be a hindering factor resulting in a reduced agglomeration by controlling the interaction between the nanoparticle.

Table 1. Lattice constant values (in Å) and crystallite size with different Co : SDS ratio at 250℃ and 500℃ of cobalt ferrite.

Annealing temperature (°C)	Co: SDS ratio	d_x (gcm^{-3})	Lattice constant 'a' (Å)		Crystallite size D (nm)		Unit cell volume V ($Å^3$)		Specific Surface area S ($Å^2$)	
			Experimental	Rietveld	$D_{Scherer}$	$D_{W\text{-}H\ plot}$	Experimental	Rietveld	Experimental	Rietveld
250	1:0.33	5.315	8.3705	8.3671	12.29	12.99	586	576	91.8	86.8
	1:0.5	5.314	8.3709	8.3758	11.74	12.73	586	587	96.1	88.6
	1:0.66	5.315	8.3702	8.3641	10.28	10.19	586	583	109.7	110.7
500	1:0.33	5.310	8.3725	8.3751	17.65	20.45	587	589	63.9	55.2
	1:0.5	5.311	8.3722	8.3768	13.33	18.39	587	579	84.7	61.4
	1:0.66	5.311	8.3723	8.3646	13.14	18.07	587	586	85.9	62.5

Fig. 7, 8, and 9 (a to c) shows Transmission electron micrographs (TEM) of cobalt ferrite with varying Co: SDS ratio at different annealing temperatures. Fine and uniform particles were observed using TEM pictures.

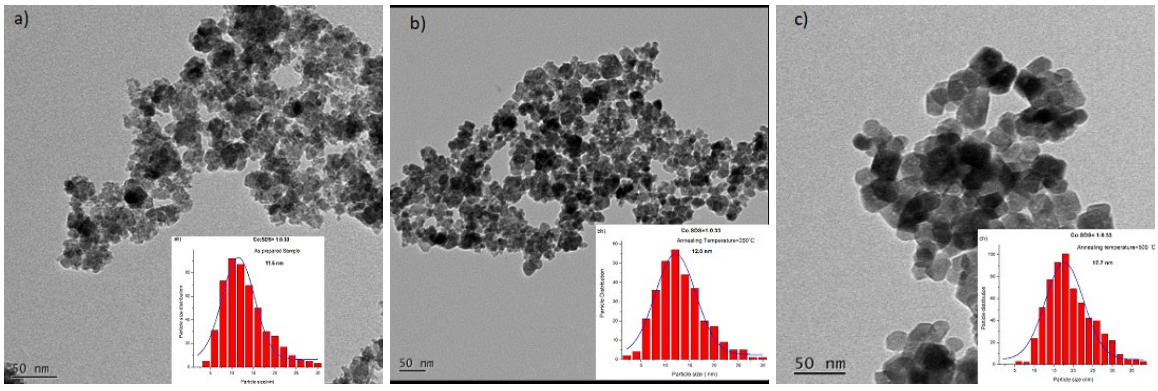

Fig. 7. TEM (a-c) with inset of histograms (particle size) samples with Co: SDS =1:0.33.

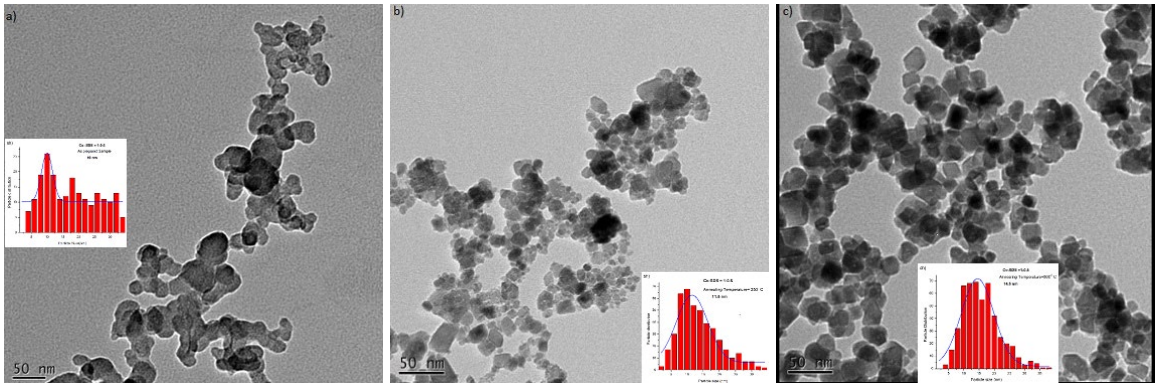

Fig. 8. TEM (a-c) with inset of histograms (particle size)samples with Co: SDS =1:0.5.

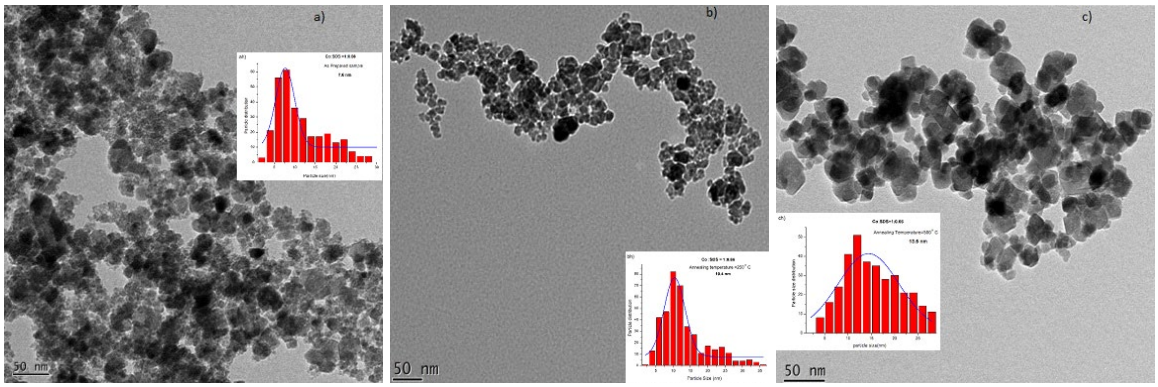

Fig. 9. TEM (a-c) with inset of histograms (particle size) samples with Co: SDS =1:0.66.

The particle size (average) was calculated for a sample using images of TEM. The particle size distribution chart was created with Gaussian function and we computed the mean particle size to arrive at the results shown in Fig. 7, 8, and 9. The histogram of the distribution is displayed for each sample at 250°C and 500°C. The annealing process is observed to increase average particle size (Table 2) as it reduces lattice defects and strains, leading to the merging of crystallites [34–36].

Table 2. Cobalt ferrite particle size with different Co : SDS ratio at different annealing temperatures.

Co: SDS ratio	Annealing temperature	Particle size (nm)
1:0.33	as-prepared	11.5
	250	12.0
	500	17.7
1:0.5	as-prepared	10.0
	250	11.5
	500	14.5
1:0.66	as-prepared	7.6
	250	10.4
	500	13.5

Between SDS concentration and particle size, there is an inverse correlation observed, indicating that excess SDS causes positive entropy due to SDS adsorption. This leads to a compensatory measure to reduce entropy, causing a decrease in particle size. This observation is consistent with previous studies [17, 37]. The nearly proportionate relationship between the average particle size (TEM) and estimated crystallite size (XRD) indicates the single domain nature of all the samples [38, 39].

Fig. 10a and b shows the magnetic hysteresis loops (room temperature) of cobalt ferrites with different Co to SDS ratios at annealing temperatures of 250°C and 500°C . As previously reported, the samples demonstrate ferromagnetic behavior with lower particle sizes. [35].

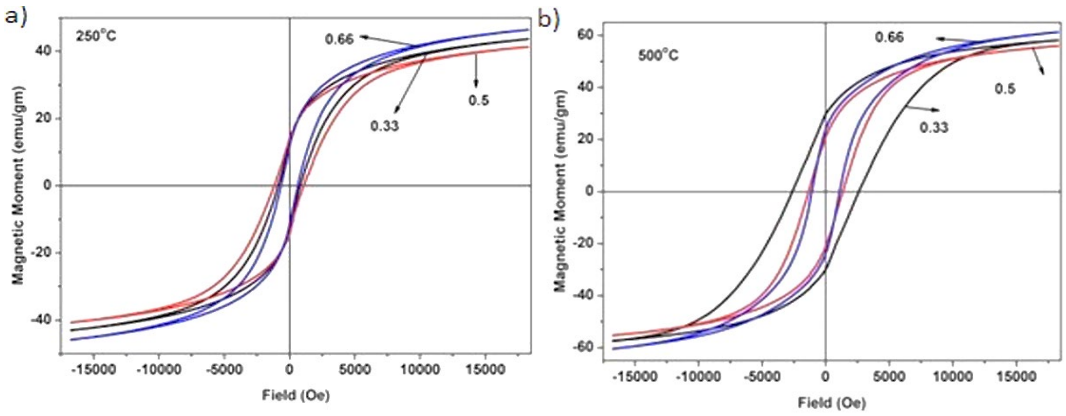

Fig. 10. Cobalt ferrite hysteresis loops with different SDS concentration at 250℃ and 500℃.

The magnetic properties, Ms, Mr, Hc, K , Mr/Ms are shown in Table 3. All samples had a squareness ratio (R) of remanence to saturation magnetization (Mr/Ms) substantially below 0.5, that demonstrates that particles have a strong magnetic interaction [34].

The present work shows that Ms value increases with rising annealing temperature and particle size as per previous studies [40].

In this work, sample containing larger SDS concentration of 1:0.66 has the largest Ms value but reports the lowest Hc value at both the annealing temperature. This decrease in Hc value at higher concentration of SDS could be the result of higher surface disorder caused by smaller particle size [27]. The high coercivity values reported by this paper, make them a good candidate for longitudinal magnetic recording media applications [41].

Table 3. Magnetic parameters of cobalt ferrite from hysteresis loop with ratio Co: SDS at different annealing temperatures.

Annealing temperature (°C)	Co: SDS ratio	Wave number ν_t (cm^{-1})	Saturation magnetization M_s (emu/g)	Retentivity M_r (emu/g)	Coercivity H_c (Oe)	Squareness ratio M_r/M_s	Magnetic anisotropy K_1 x10^6(erg/cm^3)
250	1:0.33	592	43.10	12.70	836	0.290	0.09926
	1:0.5	592	41.20	13.87	1099	0.336	0.08608
	1:0.66	592	46.16	11.31	658	0.245	0.11864
500	1:0.33	593	57.68	29.19	2617	0.500	0.13686
	1:0.5	593	55.77	21.19	1379	0.379	0.10491
	1:0.66	593	61.11	23.61	1113	0.386	0.13887

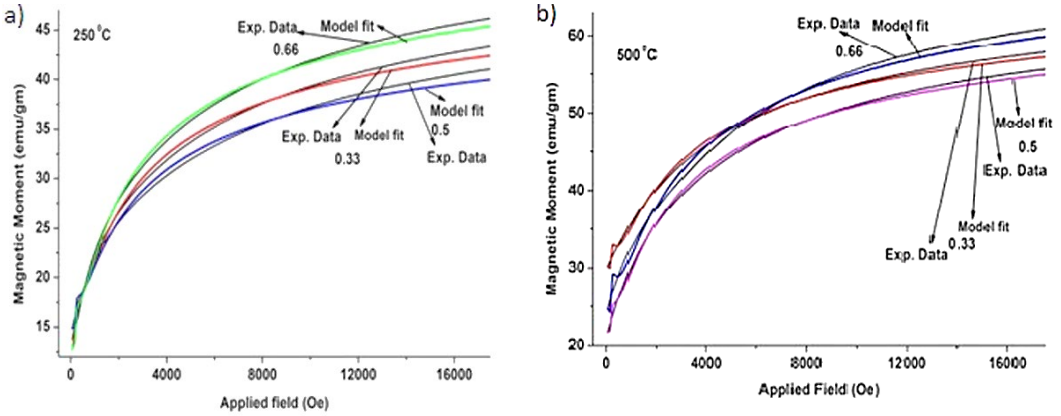

Fig. 11. Cobalt ferrite samples M-H experimental data fitting with varying SDS concentration at 250℃ and 500℃.

To understand magnetization behavior, Law of Approach to Saturation Magnetization model [42-44] has been fitted to magnetic curves and Fig 11a and 11b shows the fitting for the samples. The anisotropy constant was calculated from the fitting method and listed in Table 3.

The magnetization curve depicts that the saturation remains unachieved even though an external magnetic field up to 1.6T has been applied. The tiny particle sizes of the produced samples could be the cause of this. As the size of the particle reduces, the surface anisotropy becomes predominant, thermal effects will become dominant at room temperature in such a case as well, and due to this, saturation cannot be achieved at room temperature. With an increase in particle size, saturation effects are noted, this is also visible from rise in M_s and a fall in H_c values. Table 3 shows a positive and direct correlation between the anisotropy value and the annealing temperature.

Table 4. Cobalt ferrite samples anisotropy constant synthesized at 250℃ and 500℃ by various synthesis method.

Synthesis	Annealing Temperature °C	Anisotropy constant(K_1) x 10^6 erg/cm^3	Reference
Sol-gel	350 500	0.050 2.750	[35]
Co-precipitation method	600	3.860	[36]
Citrate Method	200 400 600	0.138 0.843 2.210	[45]
Co-precipitation method	200 400 600	0.100 0.388 1.010	[45]

The magnetic anisotropy values of this study are smaller compared to the findings for Cobalt ferrite in Table 4, which may be because of the superior saturation magnetization observed for a smaller particle size and is also supported by low squareness ratios. Cobalt ferrite exhibits a more amorphous nature at low SDS concentrations, whereas at 1:0.66 SDS concentrations, better crystallinity of cobalt ferrite without any amorphous nature is the cause of the increase in magnetic anisotropy and saturation magnetization. As per XRD Pattern, the crystallinity of cobalt ferrite is lower at 250°C annealing temperature, which accounts for the low saturation magnetization, retentivity, and coercivity values reported above.

4. Conclusion

The purpose of this preliminary investigation was to establish the optimal amount of SDS surfactant needed to synthesize crystalline cobalt ferrite and to evaluate its influence on the structural and magnetic characteristics. The interplanar spacing (d-values) and lattice constants of the cobalt ferrites were compatible with the reported values, according to XRD investigations. The average particle size determined from TEM images increased with increasing temperature and reduced with rise in the content of SDS.

Additionally examined were the produced cobalt ferrite's magnetic properties. Higher coercivity values obtained in this study could imply the presence of a single-domain nature in the material, which can be linked to better spin alignment. The squareness ratios of all samples were less than 0.5, indicating strong magnetic interaction between particles. High magnetization (Ms) and coercivity (Hc) values from M-H-loop make these materials a potential candidate for use as longitudinal magnetic recording media.

Our research emphasizes the importance of surfactant SDS in influencing and controlling the structural and magnetic properties of synthesized cobalt ferrite nanoparticles. All our results show that by careful adjustment of the synthesis conditions we can identify the ideal SDS concentration and a right annealing temperature for synthesizing the above said crystalline nanoparticles. This study's findings could have far-reaching ramifications for the design and production of other functional nanomaterials with desired features.

Acknowledgements

Dr GSVRK Choudary expresses his gratitude to UGC-SERO, Hyderabad for providing infrastructural facility (equipment) support through Minor Research Project No. FMRP-6812/2017-18 (SERO/UGC).

Authors would also like to thank the Department of Physics, GSS, GITAM (Deemed to be University) for offering their DSC facility through DST-FIST, India, for utilization of facilities-(equipment) through No.SR/FST/PSI-194/2014 Dated: 21st July 2015.

We also would like to declare that there was no specific grant received from any funding agencies in the sectors of public, commercial, or not-for-profit for this research.

References

[1] S. R. Naik, A.V. Salker, Journal of Materials Chemistry, 22,(6), 2740(2012); https://doi.org/10.1039/C2JM15228B

[2] D. Bahadur, J .Giri, B. Nayak, B., Sriharsha, T., Pradhan, P., Prasad, N. K., K.C. Barick, Ambashta, R. D., Pramana 65, 663 (2005); https://doi.org/10.1007/BF03010455

[3] A.K. Gupta, M .Gupta, biomaterials, 26(18), 3995 (2005); https://doi.org/10.1016/j.biomaterials.2004.10.012

[4] B.E. Kashevsky, V. E. Agabekov, S. B. Kashevsky, K. A. Kekalo, E. Y. Manina, I. V. Prokhorov, V. S. Ulashchik, Particuology, 6(5), 322(2008); https://doi.org/10.1016/j.partic.2008.07.001

[5] R. Jain, S. Kumar, S. K. Meena, 12 (9), 095109(2022); https://doi.org/10.1063/5.0098157

[6] Shyamaldas, M. Bououdina, C. Manoharan, Journal of Magnetism and Magnetic Materials, 493, 165703(2020); https://doi.org/10.1016/j.jmmm.2019.165703

[7] I. H. Gul, A. Maqsood, M. Naeem, M. N. Ashiq, Journal of alloys and compounds, 507(1), 201 (2010); https://doi.org/10.1016/j.jallcom.2010.07.155

[8] S. Amiri, H. Shokrollahi, Materials Science and Engineering: C, 33(1), 1(2013); https://doi.org/10.1016/j.msec.2012.09.003

[9] A. M. Kumar, M. C. Varma, C. L. Dube, K. H. Rao, S. C. Kashyap, Journal of Magnetism and

Magnetic Materials, 320(14), 1995(2008); https://doi.org/10.1016/j.jmmm.2008.02.129
[10] Zhang, Yue, Zhi Yang, Di Yin, Yong Liu, Chun Long Fei, Rui Xiong, Jing Shi, GaoLin Yan, Journal of Magnetism and Magnetic Materials, 322(21), 3470(2010); https://doi.org/10.1016/j.jmmm.2010.06.047
[11] M. A. Malik, M. Y Wani, M. A. Hashim, Arabian journal of Chemistry 5(4), 397(2012); https://doi.org/10.1016/j.arabjc.2010.09.027
[12] V. U. K. Uskokovic, M. Drofenik., Surface Review and Letters, 12(02), 239 (2005); https://doi.org/10.1142/S0218625X05007001
[13] M. P. Pileni, Journal of Experimental Nanoscience 1(1), 13(2006); https://doi.org/10.1080/17458080500462075
[14] J. Eastoe, M. J. Hollamby, L. Hudson, Advances in colloid and interface science,128, 5(2006); https://doi.org/10.1016/j.cis.2006.11.009
[15] M. P. Pileni, The Journal of physical chemistry 97 (27), 6961(1993); https://doi.org/10.1021/j100129a008
[16] I. H. Lone, N. R. Radwan, J. Aslam, A. Akhter, Current Nanoscience, 15(2),129(2019); https://doi.org/10.2174/1573413714666180611075115
[17] M. Gupta, A. Das, S. Mohapatra, D. Das, A. Datta, Applied Physics A 126,1(2020); https://doi.org/10.1007/s00339-019-3176-6
[18] A. Tavakoli, M. Sohrabi, A. Kargari, chemical papers, 61(3), 151(2007); https://doi.org/10.2478/s11696-007-0014-7
[19] V. Pillai, D. O. Shah,163 (1-2), 243(1996); https://doi.org/10.1016/S0304-8853(96)00280-6
[20] C. Singh, S. Jauhar,V. Kumar, J. Singh, S. Singhal, Materials Chemistry and Physics 156 ,188 (2015); https://doi.org/10.1016/j.matchemphys.2015.02.046
[21] M. Goodarz Naseri, E. B. Saion, H. Abbastabar Ahangar, A. H. Shaari, M. Hashim, Journal of Nanomaterials, 1(2010); https://doi.org/10.1155/2010/907686
[22] A. Das, K. K. Bestha, P. Bongurala, V. Gorige, Nanotechnology, 31(33), 335716(2020); https://doi.org/10.1088/1361-6528/ab8fe8
[23] U. B. Sontu, F. C. Chou, Journal of Magnetism and Magnetic Materials, 452, 398(2018); https://doi.org/10.1016/j.jmmm.2018.01.003
[24] R. Safi, A. Ghasemi, R. Shoja-Razavi, M. Tavousi, Journal of Magnetism and Magnetic Materials, 396, 288 (2015); https://doi.org/10.1016/j.jmmm.2015.08.022
[25] E. Hutamaningtyas, A.T. Wijayanta, B. Purnama, Journal of Physics: Conference Series , 776, (1,012023), (2016); https://doi.org/10.1088/1742-6596/776/1/012023
[26] A. M. El Nahrawy, G A Soliman, E. M. M. Sakr, H. A. El Attar, Journal of Ovonic Research, 14(3) (2018).
[27] M. Vadivel, R. R. Babu, M. Arivanandhan, K. Ramamurthi, Y. Hayakawa, RSC Adv. 5, 27060(2015); https://doi.org/10.1039/C5RA01162K
[28] S. Rana, J. Philip, Raj, Materials Chemistry and Physics, 124 (1), 264(2010); https://doi.org/10.1016/j.matchemphys.2010.06.029
[29] K. S. Rao, G. S. V. R. K Choudary, K. H. Rao, C. Sujatha, Procedia Materials Science, 10, 19(2015); https://doi.org/10.1016/j.mspro.2015.06.019
[30] J. P. K. Chintala, S. Bharadwaj, M. C. Varma, G. S. V. R. K. Choudary, Journal of Physics and Chemistry of Solids, 160, 110298(2022); https://doi.org/10.1016/j.jpcs.2021.110298
[31] S. M. A. Ridha, H. A. Khader, Turkish Journal of Computer and Mathematics Education (TURCOMAT), 12(14) 675(2021); https://doi.org/10.17762/turcomat.v12i3.773
[32] G. K. Williamson, W. H. Hall, Acta mettalurgica,1(1), 22(1953); https://doi.org/10.1016/0001-6160(53)90006-6
[33] K .Ratnaih, N. V. K Prasad., M. C. Varma, G. S. V. R. K. Choudary, Journal of Ovonic Research, 17(6) , (2021); https://doi.org/10.15251/JOR.2021.176.559
[34] W. S. Chiu, S. Radiman, R. Abd-Shukor, M. H. Abdullah, P. S. Khiew, Journal of Alloys and Compounds, 459(1-2), 291(2008); https://doi.org/10.1016/j.jallcom.2007.04.215

[35] K. S. Rao, S. R. Nayakulu, M. C. Varma, G. S. V. R. K Choudary, K. H. Rao, Journal of Magnetism and Magnetic Materials, 451, 601(2018); https://doi.org/10.1016/j.jmmm.2017.11.009
[36] K. Maaz, A. Mumtaz, S. K. Hasanain, A. Ceylan, Journal of magnetism and magnetic materials, 308 (2), 289(2007); https://doi.org/10.1016/j.jmmm.2006.06.003
[37] D. V. Leff, P. C. Ohara, J. R. Heath, W. M. Gelbart, The Journal of Physical Chemistry, 99(18),7036(1995); https://doi.org/10.1021/j100018a041
[38] G. R. Patta, V. R. Kumar, B. V. Ragavaiah, N. Veeraiah, Physics A, 126, 1(2020); https://doi.org/10.1007/s00339-019-3253-x
[39] A. Hossain, M. S. I. Sarker, M. K. R. Khan, F. A. Khan, M. Kamruzzaman, M. M. Rahman, Applied Physics A, 124, 1(2018); https://doi.org/10.1007/s00339-017-1423-2
[40] P. Laokul, S. Arthan, S. Maensiri, E. Swatsitang, Journal of Superconductivity and Novel Magnetism, 28, 2483(2015); https://doi.org/10.1007/s10948-015-3068-8
[41] G. Mustafa, I. Ahmed, M. U. Subhani, M. Shabaz, M. Iqbal, Enam-ul-Haq, R. Mehmood, Journal of Ovonic Research Vol, 17(3), 231 (2021); https://doi.org/10.15251/JOR.2021.173.231
[42] W. F. Brown Jr, Physical Review, 58(8), 736(1940); https://doi.org/10.1103/PhysRev.58.736
[43] G. F. Dionne, IEEE transactions on magnetics 39(5), 3121(2003); https://doi.org/10.1109/TMAG.2003.816026
[44] H. Hauser, D. C. Jiles, Y. Melikhov, L. Li, R. Grössinger, Journal of Magnetism and Magnetic Materials, 300(2), 273(2006); https://doi.org/10.1016/j.jmmm.2005.05.017
[45] L. Kumar, M. Kar, IEEE transactions on magnetics, 47(10), 3645(2011); https://doi.org/10.1109/TMAG.2011.2151841